http://ansinet.com/itj

ITJ

ISSN 1812-5638

INFORMATION TECHNOLOGY JOURNAL

ANSInet
Asian Network for Scientific Information
308 Lasani Town, Sargodha Road, Faisalabad - Pakistan

Information Technology Journal 11 (8): 971-979, 2012
ISSN 1812-5638 / DOI: 10.3923/itj.2012.971.979

Controller Design for an Uncertain Contactless Power Transfer System

Yan-Ling Li, Yue Sun and Xin Dai
College of Automation, Chong-Qing University, Chong-Qing, China

Abstract: This study aims to effectively restrain the effect of parametric perturbations on operating performance for Contactless Power Transfer (CPT) system. A generalized state-space averaging method based on frequency domain decomposition is applied. By this method, CPT system is approximately a linear time-invariant system and then a linear fractional transformation of GSSA model and its parametric uncertainties is discussed to generate a linear dynamic system with the perturbed feedback. Aimed at this generalized system with the structured parametric uncertainties, the D-K iteration method is proposed for designing a μ-synthesis controller based on the Structured Singular Value (SSV).The simulation and experimental results show that μ-synthesis control system has a certain dynamic performance and robustness and can not only rapidly restrain the effect of frequency and load perturbations on the system itself but also accurately track the steady value of output voltage. The results also verify that μ-synthesis method is effective for the CPT technology.

Key words: Contactless power transfer system, generalized state-space averaging method, linear fractional transformation, μ-synthesis, robustness

INTRODUCTION

Contactless Power Transfer (CPT) technology utilizes high frequency magnetic coupling to realize wireless energy transfer in short distance. Since there doesn't exit electric contact in the power transfer process, the CPT technology has been widely used in special power utilization environments such as inflammable, explosive, humid and underwater environments. Furthermore, it can provide flexible power supply for biomedical and medical devices and electric transportation vehicles. In the last decade, CPT technology has attracted more and more attention from power electronics researchers (Chaoui *et al*., 2005; Ghariani *et al*., 2006; Hmida *et al*., 2007; Casanova *et al*., 2009; Kissin *et al*., 2009; Keeling *et al*., 2010; Low *et al*., 2010; Moradewicz and Kazmierkowski, 2010).

In CPT system, due to parameter variations, especially for the disturbance on frequency and load parameter, system performances which include power transfer efficiency and distance will drop accordingly. Specially, when the frequency variation exceeds some extent, it will bring multi period operation problem (Tang *et al*., 2009) which will influence the system stability. A typical CPT system includes high frequency inverter, resonant tank, magnetic coupling and rectifier. It makes the CPT system is a typical high order nonlinear system which is easily affected by parameters disturbance.

Due to the system complexity, classic control methods mainly focus on single objective control (such as frequency and excitation current) which are independent of system model. For example, aimed at frequency stability control, dynamical and static resonant compensation methods were proposed by Ping *et al*. (2006, 2008), respectively. And a piecewise control method, which can select different control strategies according to control error and its derivative, was proposed to maintain excitation current constant (Guodong *et al*., 2008). In article of Yang *et al*. (2010), considering frequency uncertainty, a numerical iteration computing method to acquire the range of frequency variation and an EMI filter design method were proposed to maintain frequency stable. It is obvious that above methods are limited by high order, nonlinear and multi disturbance characteristics of CPT system.

At present, robust control methods (Bai *et al*., 2005; Asseu *et al*., 2008; Soltanpour *et al*., 2008; Li and Fang, 2009) for multi objectives mainly include H_∞ and μ approach. The H_∞ optimal method (Gaviria *et al*., 2005) is designed to maintain system robust stability under worst disturbance condition, which ignoring the robust performance of whole system and resulting in system conservation. The H_∞ control method is mainly designed based on non-structured uncertainty and small gain theory. While the μ-synthesis control method (Li *et al*., 2010) mainly focuses on structured uncertainty. It utilizes system structured singular value to depict the effect of

Corresponding Author: Yan-Ling Li, Lab. 1909, College of Automation, Chong-Qing University, Chong-Qing, 400030, China
Tel/Fax: +86 23 65112750

structured uncertainty on system stability and robust performance. It can solve the conservation problem brought by H_∞ control method.

Based on SP type CPT system, considering the structured uncertainty of system operation frequency and load parameter, the paper put forward a μ-synthesis controller with structured singular value. The method can improve system dynamical and robust performance under the parameter disturbance of frequency and load. The method models the whole system with Generalized State Space Averaging (GSSA) method. And the uncertainty part of the model is detached by upper fractional transformation. Furthermore, with D-K numerical iteration algorithm, a μ-synthesis output feedback controller is proposed and verified by the simulation and experimental results.

OPERATING PRINCIPLE OF SP-TYPE CPT SYSTEM

SP-type CPT system is a typical contactless power transfer system with the circuit topology of the primary side series resonance and the secondary parallel resonance, its circuit diagram can be shown in Fig. 1.

In a SP-type CPT system, the DC voltage source E_{dc} is the input. And two switching pairs (S1, S4) (S2, S3) compose high frequency inverter network. With the complementary conduction of the two switching pairs, high frequency energy is injected into the series resonant network (composed by C_P L_P and R_{Lp}). To obtain high quality sinusoidal oscillation, the zero-crossing detection of primary resonant current i_{Lp} is utilized to ensure zero-current switching condition of the inverter network. The contactless transmission of high frequency energy is realized by magnetic coupling between the primary exciting coil L_p and the secondary pickup coil L_S. In the secondary side, the parallel resonant network (composed by L_S, C_S and R_{Ls}) is utilized to produce resonance to acquire maximum power transfer. Furthermore, the high frequency energy is transformed to DC energy output with rectifier and filter (L_f, C_f).

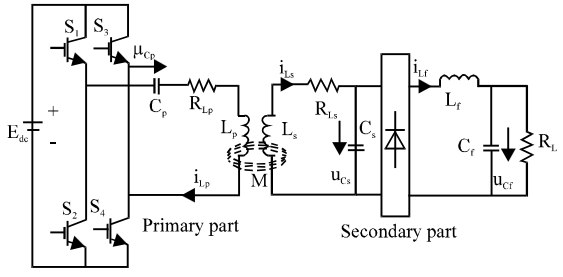

Fig. 1: Circuit topology of SP-type CPT system

To ensure maximum efficiency in the power transmission process, the inherent resonant frequency of primary series resonant network and secondary parallel resonant network should be consistent (Nayak and Reddy, 2011) and the inherent resonant frequency can be expressed as:

$$\omega_0 = 1/\sqrt{L_P C_P} = 1/\sqrt{L_S C_S} \quad (1)$$

According to the magnetic coupling principle, the RMS value of the open-circuit voltage of secondary pickup coil can be expressed as:

$$U_{OC} = \omega_0 M I_{LP} \quad (2)$$

where, ω_0 is inherent resonant frequency, I_{Lp} is the RMS value of primary resonant current, M is the mutual inductance between the primary side and the secondary side coils.

On the condition that the secondary side adopts parallel resonant network, the relation between output voltage U_O and secondary open-circuit voltage U_{OC} is approximately $U_O = Q_S U_{OC}$, which Q_S is the quality factor of load resonant circuit and can be defined as:

$$Q_S = \frac{R_L}{\omega_0 L_S} \quad (3)$$

To satisfy the power demand of load, the maximum output power should fulfill:

$$U_{OC} I_{SC} Q_S > P_O \quad (4)$$

where, I_{SC} is short-circuit current, P_O is output power of load. Therefore, short-circuit current of the secondary side should satisfy:

$$I_{SC} > \frac{P_O}{U_{OC} Q_S} \quad (5)$$

MODELING OF SP-TYPE CPT SYSTEM

The linearization approximation model of SP-type CPT system: As SP-type CPT system exhibits high order nonlinear characteristics, therefore, with GSSA method, the nonlinear model of the high frequency inverter and rectifier can be transformed to linear model.

According to Kirchhoff's voltage and current laws, the differential equation model of equivalent circuit of SP-type CPT system can be described as:

$$\begin{cases} i_{Lp}' = \Delta^{-1}(L_S R_{Lp} i_{Lp} + L_S u_{Cp} + M R_{Ls} i_{Ls} + M u_{Cs} - L_S g_1(t) E_{dc}) \\ u_{Cp}' = C_P^{-1} i_{Lp} \\ i_{Ls}' = \Delta^{-1}(M R_{Lp} i_{Lp} + M u_{Cp} + L_P R_{Ls} i_{Ls} + L_P u_{Cs} - M g_1(t) E_{dc}) \\ u_{Cs}' = C_S^{-1}(i_{Ls} - g_2(t) i_{Lf}) \\ i_{Lf}' = L_f^{-1}(g_2(t) u_{Cs} - u_{Cf}) \\ u_{Cf}' = C_f^{-1}(i_{Lf} - R_L^{-1} u_{Cf}) \end{cases} \quad (6)$$

where, $g_1(t)$ and $g_2(t)$ are binary logic switching functions, defined as:

$$g_1(t) = \begin{cases} 1 & mT < t < (2m+1)T/2 \\ -1 & (2m+1)T/2 < t < (m+1)T \end{cases}, m \in I \quad (7)$$

$$g_2(t) = g_1(t - \frac{T}{4}) \quad (8)$$

For AC signals i_{Lp}, u_{Cp}, i_{Ls}, u_{Cs}, the even harmonics are approximately zero and the odd harmonics are conjugate symmetric, when the system works close to the inherent frequency point of the LC resonant network, fundamental components of the AC signals can be used to approximate the sinusoidal oscillation components. And for DC signals i_{Lf}, u_{Cf}, zero-order harmonic component can be used to describe the steady-state characteristics and transient characteristics, the state variables can be defined as:

$$\begin{aligned} i_{Lp} &= \langle i_{Lp} \rangle_1 e^{jw_0 t} + \langle i_{Lp} \rangle_{-1} e^{-jw_0 t} \\ u_{Cp} &= \langle u_{Cp} \rangle_1 e^{jw_0 t} + \langle u_{Cp} \rangle_{-1} e^{-jw_0 t} \\ i_{Ls} &= \langle i_{Ls} \rangle_1 e^{jw_0 t} + \langle i_{Ls} \rangle_{-1} e^{-jw_0 t} \\ u_{Cs} &= \langle u_{Cs} \rangle_1 e^{jw_0 t} + \langle u_{Cs} \rangle_{-1} e^{-jw_0 t} \\ i_{Lf} &= \langle i_{Lf} \rangle_0 \\ u_{Cf} &= \langle u_{Cf} \rangle_0 \end{aligned} \quad (9)$$

Based on the differential characteristics of Fourier coefficients (Shittu and Shangodoyin, 2008) and the time-domain differential equations of the SP-type CPT system, the linear differential equations described by Fourier coefficients can be obtained as:

$$\begin{cases} \langle i_{Lp} \rangle_1' = \Delta^{-1}(L_S R_{Lp} \langle i_{Lp} \rangle_1 + L_S \langle u_{Cp} \rangle_1 + M R_{Ls} \langle i_{Ls} \rangle_1 + \\ \qquad M \langle u_{Cs} \rangle_1 - L_S \langle g_1(t) \rangle_1 E_{dc}) - j\omega_0 \langle i_{Lp} \rangle_1 \\ \langle u_{Cp} \rangle_1' = C_P^{-1} \langle i_{Lp} \rangle_1 - j\omega_0 \langle u_{Cp} \rangle_1 \\ \langle i_{Ls} \rangle_1' = \Delta^{-1}(M R_{Lp} \langle i_{Lp} \rangle_1 + M \langle u_{Cp} \rangle_1 + L_P R_{Ls} \langle i_{Ls} \rangle_1 + \\ \qquad L_P \langle u_{Cs} \rangle_1 - M \langle g_1(t) \rangle_1 E_{dc}) - j\omega_0 \langle i_{Ls} \rangle_1 \\ \langle u_{Cs} \rangle_1' = C_S^{-1}(\langle i_{Ls} \rangle_1 - \langle g_2(t) i_{Lf} \rangle_1) - j\omega_0 \langle u_{Cs} \rangle_1 \\ \langle i_{Lf} \rangle_0' = L_f^{-1}(\langle g_2(t) u_{Cs} \rangle_0 - \langle u_{Cf} \rangle_0) \\ \langle u_{Cf} \rangle_0' = C_f^{-1}(\langle i_{Lf} \rangle_0 - R_L^{-1} \langle u_{Cf} \rangle_0) \end{cases} \quad (10)$$

The generalized state variables of GSSA model can be detached to the real and imaginary part of the Fourier coefficients:

$$\begin{aligned} &\langle i_{Lp} \rangle_1 = x_1 + jx_2 \ \langle u_{Cp} \rangle_1 = x_3 + jx_4 \ \langle i_{Ls} \rangle_1 = x_5 + jx_6 \\ &\langle u_{Cs} \rangle_1 = x_7 + jx_8 \ \langle i_{Lf} \rangle_0 = x_9 \ \langle u_{Cf} \rangle_0 = x_{10} \end{aligned} \quad (11)$$

On the basis of convolution property of Fourier coefficients, the generalized state space averaging model of system can be established by linearizing the nonlinear switching term of Eq. 10:

$$\dot{x} = \tilde{A}x + \tilde{B}u \quad (12)$$

where, $\tilde{A}$ and $\tilde{B}$ are respectively the system matrix and control input matrix.

The uncertain model of SP-type CPT system: To restrain the influence of frequency and load perturbation for the system effectively, the uncertain model with respect to frequency and load of SP-type CPT system is established.

First, operating frequency and load parameter of system are defined as:

$$\begin{aligned} \omega &= \omega^*(1 + p_\omega \delta_\omega) \\ R_L &= R_L^*(1 + p_L \delta_L) \end{aligned} \quad (13)$$

where, ω and R_L are uncertain parameters but their variation range are bounded. ω^* and R_L^* are the nominal values of frequency and load parameter, respectively, $p_\omega\delta_\omega$ and $p_L\delta_L$ represent perturbation range of frequency and load parameter, respectively, where δ_ω and δ_L are normalized uncertain parameters, namely satisfy $\|\delta_\omega\| \le 1$, $\|\delta_L\| \le 1$, p_ω and p_L which directly determine system performance, are coefficients of uncertain parameters δ_ω and δ_L, respectively. The parameter uncertainty model of CPT system is to separate two uncertain parameters δ_ω and δ_L from the linear approximation model of system.

The frequency and load parameter can be expressed in the form of upper linear fractional transformation $\omega = F_U(M_\omega, \delta_\omega)$:

$$\frac{1}{R_L} = F_U(M_L, \delta_L)$$

system structure with upper fractional transformation can be shown in Fig. 2.

where, both M_ω and M_L are invariant transfer function matrixes, respectively are:

$$M_\omega = \begin{bmatrix} 0 & \omega^* \\ p_\omega & \omega^* \end{bmatrix} \quad (14)$$

$$M_L = \begin{bmatrix} -p_L & 1/R_L^* \\ -p_L & 1/R_L^* \end{bmatrix} \quad (15)$$

The input and output of uncertain parameters δ_ω and δ_L can be expressed as $y_{i\omega}$, $u_{i\omega}$ and y_{jL}, u_{jL}, are x_i and x_j are system state variables, hence there exist $v_{i\omega} = x_i\omega$, $v_{jL} = x_j/R_L$. M_ω and M_L both have 2 inputs and 2 outputs, the relationship between input and output can be expressed as:

$$\begin{bmatrix} y_{i\omega} \\ v_{i\omega} \end{bmatrix} = \begin{bmatrix} 0 & \omega^* \\ p_\omega & \omega^* \end{bmatrix} \begin{bmatrix} u_{i\omega} \\ x_i \end{bmatrix} = \begin{bmatrix} \omega^* x_i \\ p_\omega u_{i\omega} + \omega^* x_i \end{bmatrix} \quad (16)$$

$$\begin{bmatrix} -p_L & 1/R_L^* \\ -p_L & 1/R_L^* \end{bmatrix} \begin{bmatrix} u_{jL} \\ x_j \end{bmatrix} = \begin{bmatrix} -p_L u_{jL} + x_j/R_L^* \\ -p_L u_{jL} + x_j/R_L^* \end{bmatrix} \quad (17)$$

By separating uncertain parameters δ_ω and δ_L relating to each state variables, uncertain matrix Δ of SP-type CPT system can be obtained as:

$$\Delta = \text{diag}\ \{\delta_\omega, \ldots, \delta_\omega, \delta_L\} \quad (18)$$

where, $\Delta \epsilon R^{9\times 9}$, $\bar{\sigma}(\Delta) \le 1$

And input and output of uncertain matrix Δ are used as output and input of nominal model and can be expressed as:

$$\begin{aligned} y_p &= \text{pertin} = [y_{1\omega}, y_{3\omega}, \cdots, y_{8\omega}, y_{10L}]^T \\ u_p &= \text{pertout} = [u_{1\omega}, u_{2\omega}, \cdots, u_{8\omega}, u_{10L}]^T \end{aligned} \quad (19)$$

The uncertain model of SP-type CPT system can be expressed as a linear dynamic system with perturbation feedback $G = F_U(G_{mds}, \Delta)$, as shown in Fig. 3.

In Fig. 3, G_{mds} is generalized nominal model, perturbation block Δ is uncertainty part, input vector u

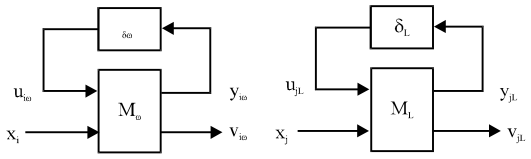

Fig. 2: Linear fractional transformation for uncertain parameters ω and R_L

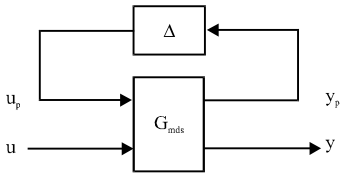

Fig. 3: Uncertain model of SP-type CPT system

includes all external signals, such as input and output perturbation, noise, reference input, etc.

The state space for generalized nominal model G_{mds} can be described as:

$$\begin{cases} \dot{x} = Ax + B_1 u_p + B_2 u \\ y_p = C_1 x + D_{11} u_p + D_{12} u \\ y = C_2 x + D_{21} u_p + D_{22} u \end{cases} \quad (20)$$

Which, $x \epsilon R^n$ is state variable, $u \epsilon R^m$ is control input, $y \epsilon R^r$ is measured output (load output voltage), $u_p \epsilon C^p$ and $y_p \epsilon C^p$ are external signals of model uncertainty.

μ-SYNTHESIS CONTROLLER DESIGN

In SP-type CPT system, to overcome the influence to system performance from frequency, load perturbation and output disturbance, the output feedback controller based on μ-synthesis method u(s) = K (s)e(s) can be shown in Fig. 4.

In the figure, ref is reference value of load output voltage in; G_{mds} is generalized nominal object model; Δ is norm-bounded structured uncertainty block; d is load output disturbance with limited energy, that is $d \epsilon L_2$; W_p and W_u are performance weighting functions They reflect robust performance requirements at different frequency.

μ-synthesis problem: First closed-loop control system can be transformed into the standard linear fractional description for μ-synthesis control, as shown in Fig. 5.

$Z = [e_p, e_u]^T$ is controlled output, P represents open-loop connection, including generalized nominal model and performance weighting function; $\hat{\Delta}$ is augmented perturbation matrix composed of structured uncertainty block $\Delta \epsilon R^{9\times 9}$ and performance uncertainty block $\Delta_p \epsilon C^{1\times 2}$:

$$\hat{\Delta} = \left\{ \begin{bmatrix} \Delta & 0 \\ 0 & \Delta_p \end{bmatrix} : \|\Delta\|_\infty \le 1,\ \|\Delta_p\|_\infty \le 1 \right\} \quad (21)$$

μ-synthesis for system robust stability and performance is to find a steady controller K, such that:

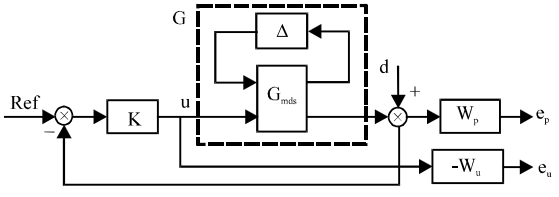

Fig. 4: Block diagram of μ-synthesis control system

$$\sup_{\omega \in R} \mu_{\hat{\Delta}}[M(P,K)(j\omega)] < 1 \quad (22)$$

Considering the optimal case, above problem can be attributed to find the minimum amplitude and frequency peak value of $\mu_{\hat{\Delta}}(\cdot)$ for closed-loop transfer function M (s) in all steady controllers K, that is:

$$\inf_{K(s)} \sup_{\omega \in R} \mu_{\hat{\Delta}}[M(P,K)(j\omega)] \quad (23)$$

When solving μ-synthesis problem in practice, upper bound of μ can be used to replace $\mu_{\hat{\Delta}}(\cdot)$, according to theorems (Kemin *et al*., 1996) and μ-synthesis problem can be further described as:

$$\inf_{K(s)} \inf_{D \in \underline{D}} \left\| DM(P,K)(j\omega)D^{-1} \right\|_\infty \quad (24)$$

where, $D \in \underline{D}$ called metric matrix and set $\underline{D}$ is defined as:

$$\underline{D} = \{\text{diag}(D_1, \cdots, D_s, d_1 I_{m_1}, \cdots, d_f I_{m_f}) :$$
$$D_i \in C^{n_i \times n_i}, D_i = D_i^* > 0, d_j \in R, d_j > 0\}$$

μ-synthesis controller: The effective approximate method for solving the μ-synthesis problem is D-K iterative algorithm, its principle is to alternately the minimize Eq. 24 with fixing metric matrix D and controller K, respectively.

The first step of D-K iteration is to select D (s) = 1, an output feedback controller is solved. However, within the frequency range of [10^{-2}, 10^{6}], the peak value of μ for closed-loop system reaches 118.004, which will dissatisfy the design requirements for robust stability and robust performance.

By going on with D-K iteration, the robustness of system is continuously improved until there exit μ<1 in the entire frequency band of [10^{-2}, 10^{6}]. The result at tenth iteration is shown in Fig. 6.

Obviously, in the observed frequency range, the amplitude-frequency curves of the μ value in closed-loop system are always below 1, which indicate the robust performance requirements are met under the μ-synthesis control. In the frequency range of [10^{-2}, 10^{6}], the peak value of μ is 0.571, indicating that to maintain the stability of closed-loop system, the permissible perturbation are $\|\Delta\|_\infty$<1/0.571 with structured parameter uncertainty.

In the process of D-K iteration, characteristic parameters of controller and D-matrix are shown in Table 1.

As it can be seen, with every iteration, μ-value and γ-value of closed-loop system decrease accordingly, indicating that the robustness of system is improved constantly; the order of μ-controller is directly related to metric matrix D, after the tenth iteration, the order of μ-controller will be 46, it is necessary to reduce the order for the controller.

The contrast frequency response curves of μ-controller before and after reduced-order are shown in Fig. 7. It can be seen that the two frequency response curves are consistent.

Table 1: Iteration parameters

Iteration	Controller order	Total D-scale order	γ achieved	Peak μ value
1	12	0	950	118
5	108	96	16.8	2.43
7	76	64	14. 4	1.18
10	46	34	8.28	0.571

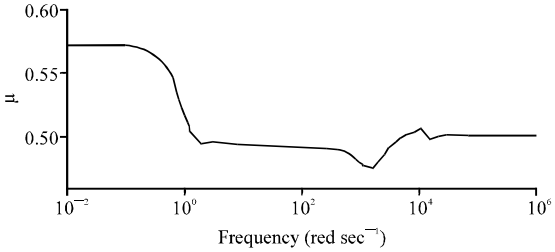

Fig. 6: μ values at 10th iteration

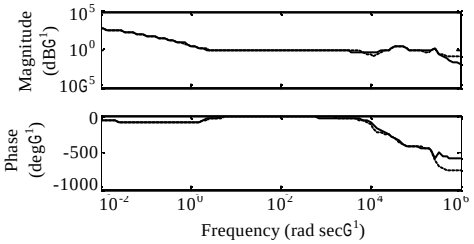

Fig. 7: Frequency response curves of full-and reduced-order controllers (46 order-real line, 8 order-dash line)

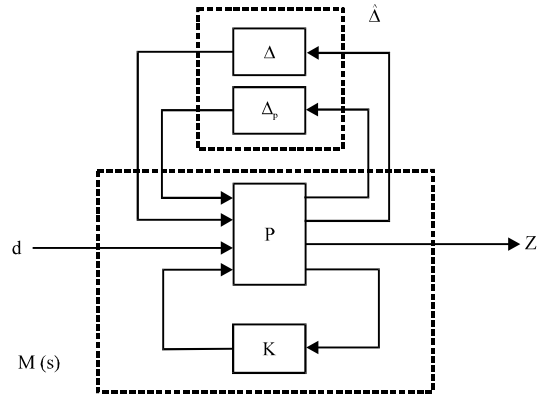

Fig. 5: Standard block diagram of μ-synthesis control system

It should be noted here that the solving result of D-K iterative algorithm only is the optimal solution in the frequency band of $[10^{-2}, 10^{6}]$, hence the designed μ-synthesis controller can't guarantee a global optimal solution but its effectiveness has been verified by coming simulation and experimental results.

EXPERIMENTAL AND SIMULATION RESULTS

According to the operating principle of SP-type CPT circuit, the main circuit parameters for the simulation are shown in Table 2.

Simulation result: With the MATLAB/SIMULINK simulation platform, simulation model has been established with parameters in Table 2, shown in Fig. 8.

The voltage source E_{dc} is realized by a buck chopper. In the simulation, the output voltage is sampled and sent to discretized μ-synthesis controller. And the control output is transformed to PWM signal by PWM block to drive the buck chopper.

First, this paper simulates and analyses the startup process of SP-type CPT system. The simulation time is set at 0.05 sec, the system starts up at 0.02 sec and required output voltage of load is set at 40 V, the waveforms are shown in Fig. 9.

It can be seen from the figure that μ-synthesis controller has fast response at startup, the load output u_o can be stabilized on 40 V after a small overshoot by adjusting input voltage E_{dc}. The adjusting time is about 10 m sec. However, since buck converter exists inherent output ripple, the waveform of u_o at steady state is affected relevantly. The small overshoot of startup process and short adjusting time show the closed-loop system has a good dynamic response characteristic.

The closed-loop system's ability to restrain the perturbation of circuit parameters directly reflects the robust performance of system. Assuming that the reference value of output steady voltage is 40 V, under the condition of load perturbations: the load value is 100 Ω in the range of [0.01, 0.03) sec; the load value varied to 300 Ω in the range of [0.03, 0.05) sec; the load value reverts to 100 Ω in the range of [0.05, 0.07] sec. The system waveforms with whole load perturbations are shown in Fig. 10.

From the figure, ripple amplitudes of output voltage E_{dc} of buck converter with load perturbations are slightly different, ripple with 300 Ω load is small; the envelope of the primary resonant current i_{Lp} tends to be smooth with the reduce of ripple of E_{dc}; the current through load changes obviously, while the amplitude of output voltage

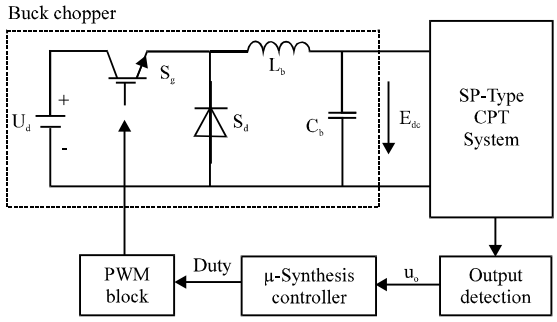

Fig. 8: Block diagram of closed-loop control system

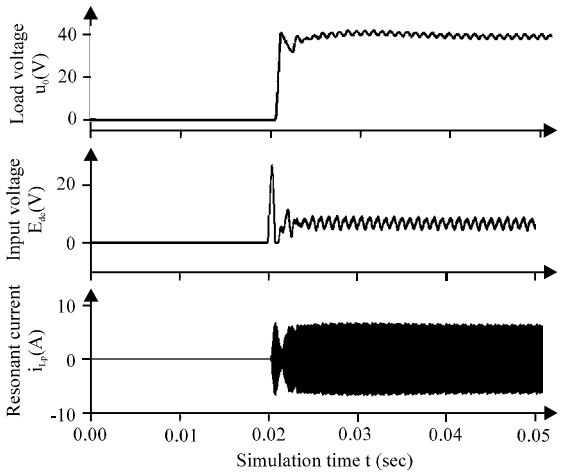

Fig. 9: System waveforms in startup process (200 Ω)

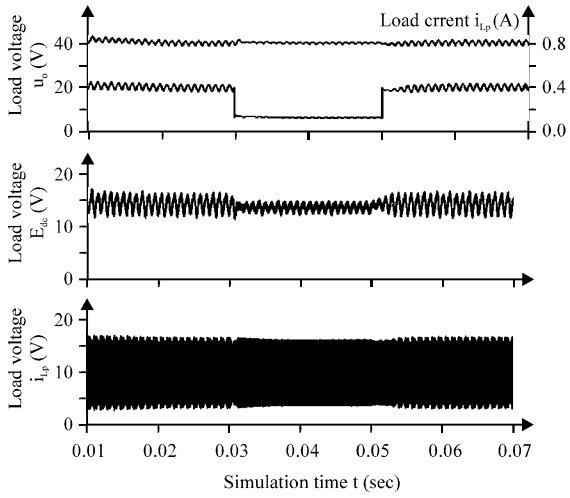

Fig. 10: System waveforms with load perturbations

Table 2: Parameters of SP-type CPT system

C_P/μF	L_P/μH	M/μH	C_S/μF
0.470	158	43.0	1.00
L_S/μH	C_f/μF	L_f/mH	R_1/Ω
74.3	22.0	1.00	200

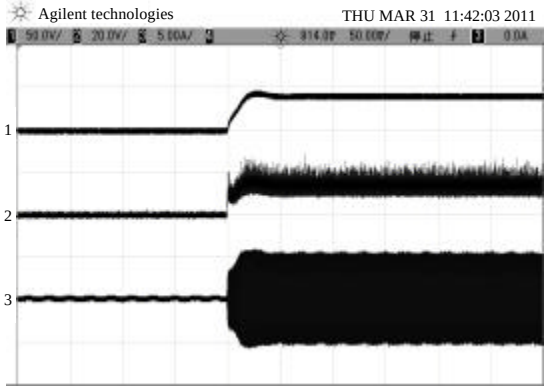

Fig. 11: Startup process of CPT system (1: u_o, 50.0 V/Div, 2: E_{dc}, 20.0 V/Div, 3: i_{Lp}, 5.00A/Div, Time: 50.00 msec/Div)

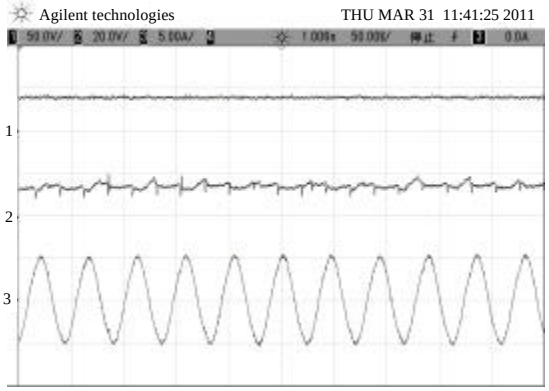

Fig. 12: Steady state of CPT system (1: u_o, 50.0 V/Div, 2: E_{dc}, 10.0 V/Div, 3: i_{Lp}, 5.00 A/Div, Time: 50.00 μsec/Div)

u_o has little change, which shows that the system output has a certain robustness for load perturbations with μ-synthesis control.

Experimental results: To verify the effectiveness of μ-synthesis controller, the experimental device of system is established on the basis of principle block diagram shown in Fig. 8. To obtain high-precision control effect and good sine wave oscillation, we use DSP (Digital Signal Processor) TMS320F2812 as the main control chip to achieve μ-synthesis discrete control algorithm; the buck chopper link uses 20 V dc-source. The system realizes steady voltage robust control of u_o by high-speed sampling, processing output voltage u_o and exporting PWM switching signals of buck link.

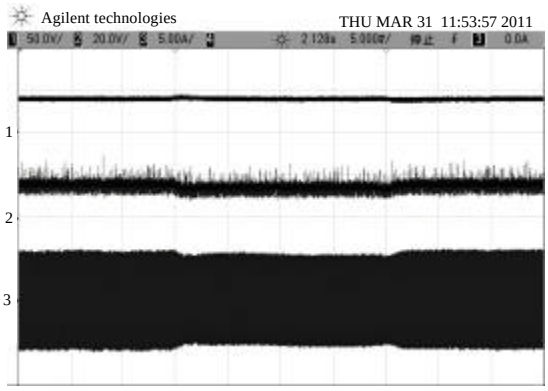

Fig. 13: Process with the load perturbations (1: u_o, 50.0 V/Div, 2: E_{dc}, 20.0 V/Div, 3: i_{Lp}, 5.00A/Div, Time: 100.00 msec/Div)

Figure 11 is circuit waveform in startup process, including output voltage u_o of load, output voltage E_{dc} of buck converter and primary resonant current i_{Lp}.

It can be seen from the Fig. 11 that u_o can be stable at 40 V after a certain overshoot with μ-synthesis controller after power on, the entire process last about 30 msec, a little longer than simulation time. Consistent with the simulation result, E_{dc} also has ripples of a certain amplitude.

To observe the waveform quality of circuit, the waveforms of steady state in Fig. 11 are expanded, as shown in Fig. 12.

Figure 12 shows output voltage u_o can be stable at about 40 V and steady state error is small although E_{dc} has a certain ripple; the primary resonant current i_{Lp} is close to standard sine wave oscillating characteristic, indicating that SP-type CPT system with μ-synthesis control has good waveform quality.

Similar to the simulation process, we study and evaluate the robust performance of system by observing the effect of load perturbation for closed-loop system. Figure 13 shows the relevant waveforms with different loads, experiment processes are divided into three steps with different load values 100, 300 and 100 Ω.

Obviously, when load value is 300 Ω (intermediate regime), the amplitude of E_{dc} and i_{Lp} decrease correspondingly. But in the entire process, output voltage u_o is barely affected by load perturbation. The experimental results are in accordance with simulation results.

In addition, the steady waveforms with different load values above are shown in Fig. 14, including output voltage u_o, PWM gate signals and primary resonant current i_{Lp}.

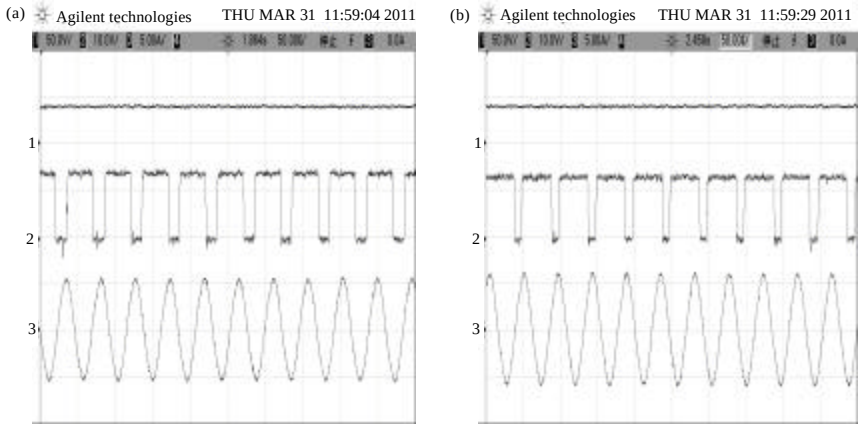

Fig. 14(a-b): Steady states of CPT system with different load values (1: u_o, 50.0 V/Div, 2: PWM signal, 10.0 V/Div, 3: i_{Lp}, 5.00A/Div, Time: 50.00 μsec/Div), (a) Steady state 1 and (b) Steady state 2

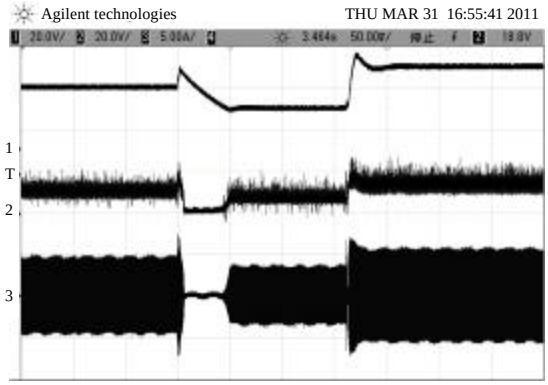

Fig. 15: Process with the reference values of steady-voltage changed (30, 20, 40 V) (1: u_o, 20.0 V/Div, 2: E_{dc}, 10.0 V/Div, 3: i_{Lp}, 5.00A/Div, Time: 200.00 msec/Div)

Figure 14 show that u_o and i_{Lp} have good waveform quality at different steady states, the duty cycle of PWM signal is basically stable: the stable duty cycle is D = 0.67 with R_L = 300 Ω; the stable duty cycle is D = 0.82 with R_L = 100 Ω.

In the application of CPT technology, to improve operating efficiency, output voltage should be varied dynamically with actual demand of loads. The reference values of output voltage 30, 20, 40 V is given successively to observe the following features of μ-synthesis control system in the experiment.

Figure 15 shows that the system can follow the variation of reference voltage value quickly with μ-synthesis control, due to this, the real-time duty cycle calculated by μ-controller is comparatively small when the reference voltage is lower which may cause zero flow of i_{Lp}. Thus, to ensure the normal operation, the minimum of duty cycle should be limited in the algorithm.

CONCLUSION

GSSA is a modeling method using low order Fourier series for approximating time-domain variables of system, which is not only suitable for dc variables with slow time-varying characteristics but also suitable for ac variables with rapid oscillation characteristics, besides, transient and steady process of electronic devices can be analyzed faster and better.

Therefore, SP-type CPT system separates uncertainty of GSSA model with GSSA modeling method by linear fractional transformation for the system uncertainty. The μ-synthesis control system designed for uncertainty of system parameters can quickly startup and accurately track the output steady voltage value of load and can restrain the effect of load perturbation for system effectively, so that the robust stability of system can satisfy certain robust performance. The simulation and experimental results have verified the feasibility of μ-synthesis method on the field of CPT.

ACKNOWLEDGMENTS

This study was supported in part by the Fundamental Research Funds for the Central Universities under Grant CDJXS11172238, by the research funds for the National Natural Science Foundation of China under Grant

50807057 and by the Specialized Research Funds for the Doctoral Program of Higher Education under Grant 20090191110021. The authors would like to thank all reviewers for their valuable comments.

REFERENCES

Asseu, O., M. Koffi, Z. Yeo, X. Lin-Shi, M.A. Kouacou and T.J. Zoueu, 2008. Robust feedback linearization and observation approach for control of an induction motor. Asian J. Applied Sci., 1: 59-69.

Bai, Z.F., S.X. Li and B.G. Cao, 2005. H_∞ control applied to electric torque control for regenerative braking of an electric vehicle. J. Applied Sci., 5: 1103-1107.

Casanova, J.J., Z.N. Low and J. Lin, 2009. A loosely coupled planar wireless power system for multiple receivers. IEEE Trans. Ind. Electron., 56: 3060-3068.

Chaoui, M., H. Ghariani, M. Lahiani and F. Sellami, 2005. An optimal geometry for power energy and data transmission in the inductive link. J. Applied Sci., 5: 1504-1513.

Gaviria, C., E. Fossas and R. Grino, 2005. Robust controller for a full-bridge rectifier using the IDA approach and GSSA modeling. IEEE Trans. Circuits Syst., 52: 609-616.

Ghariani, H., M. Chaoui, M. Lahiani, R. Perdriau and F. Sellami, 2006. Reducing load effects in high-energy, high-efficiency inductive links. J. Applied Sci., 6: 911-918.

Guodong, C., S. Yue, D. Xin and W. Zhihui, 2008. On piecewise control method of contactless power transmission system. Proceedings of the 27th Chinese Control Conference, Jul 16-18, 2008, Kunming, pp: 72-75.

Hmida, G.B., H. Ghariani and M. Samet, 2007. Design of wireless power and data transmission circuits for implantable biomicrosystem. Biotechnology, 6: 153-164.

Keeling, N.A., G.A. Covic and J.T. Boys, 2010. A unity-power-factor IPT pickup for high-power applications. IEEE Trans. Ind. Electron., 57: 744-751.

Kemin, Z., C. D. John and G. Keith, 1996. Robust and Optimal Control. Prentice Hall, New Jersey.

Kissin, M.L.G., J.T. Boys and G.A. Covic, 2009. Interphase mutual inductance in polyphase inductive power transfer systems. IEEE Trans. Ind. Electron., 56: 2393-2400.

Li, Q., W.R. Chen, S.K. Liu, Z.L. Cheng and X.Q. Liu, 2010. μ-synthesis control of proton exchange membrane fuel cell generation system based on D-K iteration method. Proceedings of the Asia-Pacific Power Energy Engineering Conference, Mar 28-31, 2010, Chengdu, pp: 1-4.

Li, X.S. and H.J. Fang, 2009. H8 controller for consensus of swarm agents with complete and incomplete communication graphs. J. Applied Sci., 10: 1929-1935.

Low, Z.N., J.J. Casanova, P.H. Maier, J.A. Taylor, R.A. Chinga, and J. Lin, 2010. Method of load/fault detection for loosely coupled planar wireless power transfer system with power delivery tracking. IEEE Trans. Ind. Electron., 57: 1478-1486.

Moradewicz, A.J. and M.P. Kazmierkowski, 2010. Contactless energy transfer system with FPGA-controlled resonant converter. IEEE Trans. Ind. Electron., 57: 3181-3190.

Nayak, D.K. and S.R. Reddy, 2011. Performance of the push pull LLC resonant and PWM ZVS full bridge topologies. J. Appl. Sci., 11: 2744-2753.

Ping, S., A.P. Hu, S. Malpas and D. Budgett, 2006. Switching frequency analysis of dynamically detuned ICPT power Pick-ups. Proceedings of the IEEE International Conference on Power System Technology, October 22-26, 2006, Chongqing, pp: 1-8.

Ping, S., A.P. Hu, S. Malpas and D. Budgett, 2008. A frequency control method for regulating wireless power to implantable devices. IEEE Trans. Biomed. Cir. Sys., 2: 22-29.

Shittu, O.I. and D.K. Shangodoyin, 2008. Detection of outliers in time series data: A frequency domain approach. Asian J. Scientific Res., 1: 130-137.

Soltanpour, M.R., M.M. Fateh and A.R. Ahmadi Fard, 2008. Nonlinear tracking control on a robot manipulator in the task space with uncertain dynamics. J. Applied Sci., 8: 4397-4403.

Tang, C., Y. Sun, Y. Su, S.K. Nguang and A.P. Hu, 2009. Determining multiple Steady-state ZCS operation points of a Switch-mode contactless power transfer system. IEEE Trans. Power Electron., 24: 416-425.

Yang, S., Q. Lei, F.Z. Peng and Z. Qian, 2010. A robust control scheme for grid-connected voltage source inverters. Proceedings of the IEEE Applied Power Electronics Conference and Exposition, February 21-25, 2010, Palm Springs, CA, pp: 1002-1009.